



Supplementary Materials

# Poly-*N*-Acetyllactosamine Neo-Glycoproteins as Nanomolar Ligands of Human Galectin-3: Binding Kinetics and Modeling

Ladislav Bumba, Dominic Laaf, Vojtěch Spiwok, Lothar Elling, Vladimír Křen and Pavla Bojarová

## Contents

1. Molecular model of Gal-3 carbohydrate recognition domain (PDB ID: 4LBN) (Figure S1)
2. Synthesis of functionalized glycans 1–8 (Scheme S1)
3. Synthesis and characterization of neo-glycoproteins 9–16 (Scheme S2, Figures S2, S3, S4)
4. Production of soluble recombinant His<sub>6</sub>-tagged galectin-3
5. ELISA-type binding assays, binding curves (Figures S5, S6)
6. Binding and inhibition properties of Gal-3-AVI (Table S1)
7. SPR sensograms and kinetic data table (Figures S7, S8, Table S2)

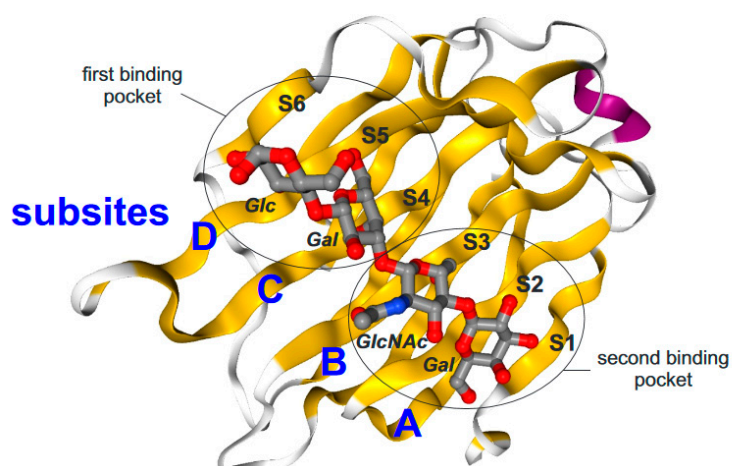
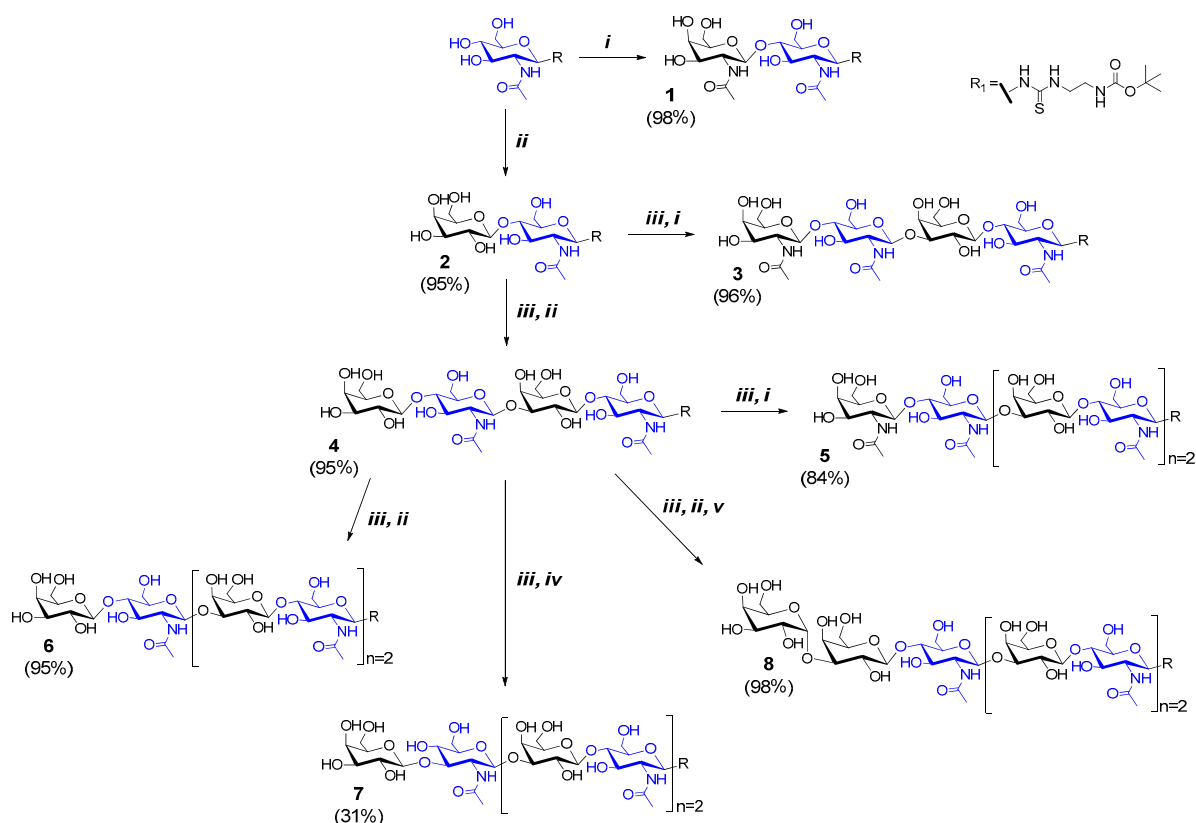
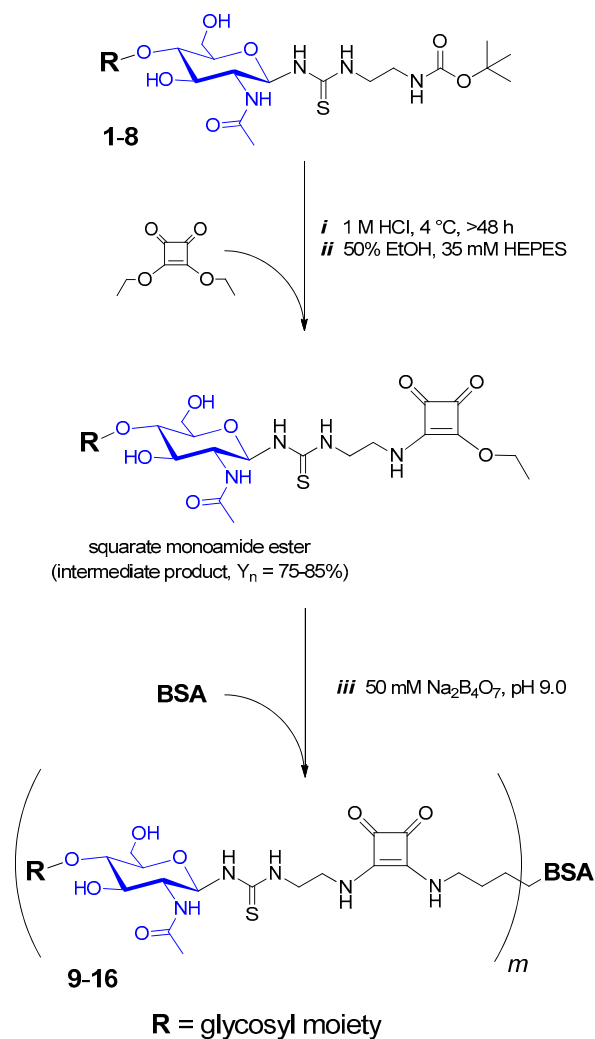


**Figure S1.** Molecular model of Gal-3 carbohydrate recognition domain (CRD) (PDB ID: 4LBN), adapted from the literature [1–3]. Lacto-*N*-neotetraose (Gal $\beta$ <sub>1,4</sub>GlcNAc $\beta$ <sub>1,3</sub>Gal $\beta$ <sub>1,4</sub>Glc) occupies both the first binding pocket ( $\beta$ -strands S<sub>4</sub>–S<sub>6</sub>) and the second binding pocket ( $\beta$ -strands S<sub>1</sub>–S<sub>3</sub>).



**Scheme S1.** Enzymatic synthesis of glycans 1-8 using mutant human  $\beta$ 4-galactosyltransferase ( $\beta$ 4GalTY284L, *i*), human  $\beta$ 4-galactosyltransferase ( $\beta$ 4GalT, *ii*), *Helicobacter pylori*  $\beta$ 3-N-acetylglucosaminyltransferase ( $\beta$ 3GlcNAcT, *iii*), *E. coli*  $\beta$ 3-galactosyltransferase ( $\beta$ 3GalT, *iv*) and murine  $\alpha$ 3-galactosyltransferase ( $\alpha$ 3GalT, *v*) according to previous reports [3-6]. All reactions were supplemented with the appropriate glycosyl acceptors (5 mM), the respective activated nucleotide sugar donors (1.5-3.0-fold molar excess of UDP-GalNAc, UDP-Gal, UDP-GlcNAc), equimolar divalent cations (*i*, *ii* and *v* =  $Mn^{2+}$ ; *iii* and *iv* =  $Mg^{2+}$ ) and alkaline phosphatase (degradation of UDP, which may inhibit glycosyltransferase reaction). The reactions were performed in aqueous buffers according to the pH optimum of each individual enzyme (*i*, *iii* and *iv* = 100 mM HEPES [pH 7.6]; *ii* = 100 mM MOPS [pH 6.8]; *v* = 100 mM MOPS [pH 6.0]) at 30 °C without shaking. After proceeded reaction, samples were heated (95 °C, 5 min), centrifuged (13,400 rpm, 10 min) and analyzed by reversed-phase HPLC (Dionex HPLC system, column: MultoKrom C18 250 mm  $\times$  4 mm; CS-Chromatographie, Langerwehe, Germany) in 15 % (*v/v*) acetonitrile in double distilled  $H_2O$  supplemented with 0.1 % (*v/v*) formic acid at a flow rate of 1 mL/min. Preparative purification was performed by solid-phase extraction (Sep-Pak C18 1/3/6cc Vac Cartridges, Waters Corporation) according to manufacturer's instructions. Alternatively, products were purified by preparative HPLC using the above conditions with MultoKrom C18 (250 mm  $\times$  20 mm, CS-Chromatographie, Langerwehe, Germany) and an adjusted flow rate of 25 mL/min.



**Scheme S2.** Synthesis of multivalent neo-glycoproteins **9–16** using diethyl squarate as a homobifunctional linker. Oligosaccharides **1–8** were deprotected under acidic conditions as indicated. The resulting primary amine was reacted with a four-fold molar excess of diethyl squarate and triethylamine in 50% aqueous ethanol (23 °C, 18 h, 400 min<sup>-1</sup> shaking frequency). The purification of squarate monoamide ester intermediate products from the crude reaction was accomplished by preparative HPLC using MultoKrom C18 (250 mm × 20 mm, CS-Chromatographie, Langerwehe, Germany) and an adjusted flow rate of 12.5 mL/min [3,4,6]. Pure intermediate products were mixed with bovine serum albumin (BSA, 0.06 mM) in 50 mM  $\text{Na}_2\text{B}_4\text{O}_7$  buffer (pH 9.0). After 7 days of incubation at 23 °C (400 min<sup>-1</sup> shaking frequency), the resulting neo-glycoproteins **9–16** were harvested by centrifugation using VivaSpin® 500 (Sartorius Stedim Biotech, Göttingen, Germany). The modification density ( $m$ ) of neo-glycoproteins **9–16** was determined by TNBSA-assay [4]. Refer to Scheme S1 for composition of glycosyl moiety residues. Neo-glycoprotein **9** carries glycans **1**, neo-glycoprotein **10** is decorated with glycan **2** and so forth (as also indicated in Table 1 in the main text).

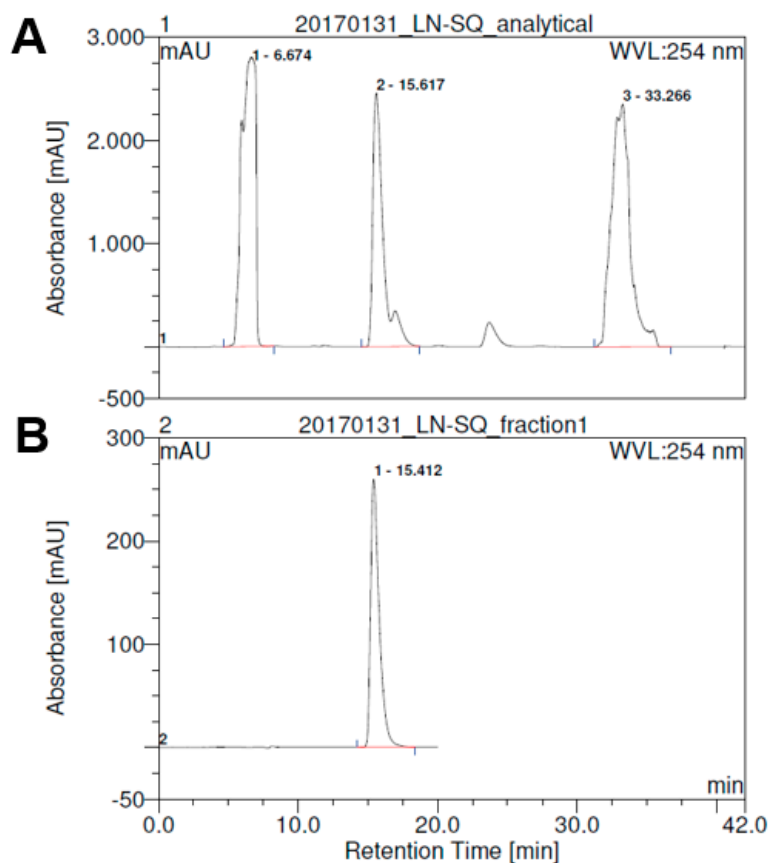


**Figure S2.** LacNAc-squarate monoamide ester before (A) and after purification by preparative HPLC (B). The reaction was monitored by reversed-phase HPLC (Dionex HPLC system, column: MultoKrom C18 250 mm  $\times$  4 mm [CS-Chromatographie, Langerwehe, Germany], 15% (v/v) acetonitrile in MilliQ-H<sub>2</sub>O, a flow rate of 0.5 mL/min). Preparative purification of squarate monoamide ester was performed by preparative HPLC under the same conditions using MultoKrom C18 (250 mm  $\times$  20 mm, CS-Chromatographie, Langerwehe, Germany) and an adjusted flow rate of 12.5 mL/min.

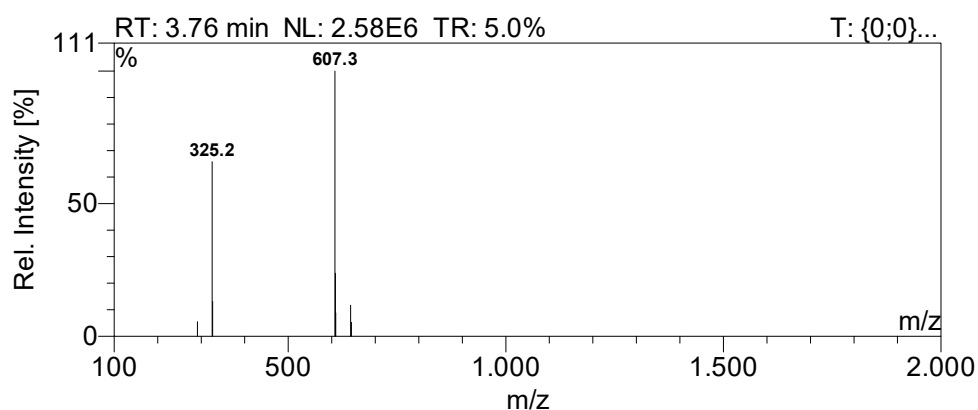


**Figure S3.** Mass spectrum of LacNAc-squarate monoamide ester. Electrospray ionization HPLC-ESI-MS and quadrupole mass analyzer (Finnigan Surveyor MSQ Plus, Thermo Scientific, needle voltage = 4 kV, temperature = 400 °C, cone voltage = 100 V, negative mode). The observed  $[M-H]^-$  of 607.3  $m/z$  corresponds well to the theoretical value of  $[M-H]^- = 607.2 m/z$ .

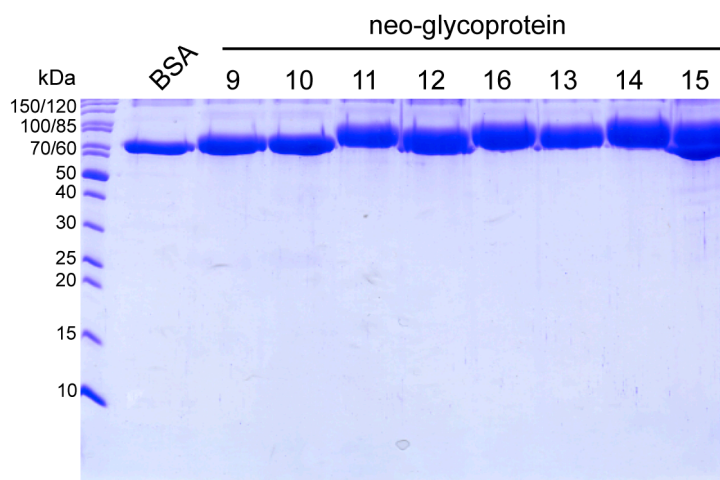


**Figure S4.** SDS-PAGE analysis of non-modified BSA and BSA neo-glycoproteins **9–16** carrying multiple glycan residues; M – PageRuler Prestained Protein Ladder (ThermoFisher Scientific). The increase of molecular weight and smearing character illustrates glycan attachment.

### Galectin-3 production

The His<sub>6</sub>-tagged human galectin-3 (Gal-3) was prepared as described previously [7]. Briefly, the gene for Gal-3 was amplified from human mesangial cDNA using the primers 5'-ATGGCAGACAATTTTCGCTCCATGATGCG-3' and 5'-TATATCATGGTATATGAAGCACTGGTGAGGTC-3'. After introduction of restriction sites for SgsI and EcoR1 using the primers 5'-GGCGCGCCTTATATCATGGTATATGAAGC-3' and 5'-CCGGAATCCGGGATGGCAGACAATTTT-3', the insert was ligated into the plasmid pETDuet-1 (Novagen, Merck, Darmstadt, Germany). The protein was recombinantly expressed in *E. coli* Rosetta (DE3) pLysS cells. Cultivation was performed in LB medium supplemented with appropriate antibiotics (130 rpm, 37 °C, 100 µg/mL ampicillin, 34 µg/mL chloramphenicol). On the next day, the one-liter main culture (TB medium, 5 L baffled flask, supplemented with respective antibiotics) was inoculated (1:10) and incubated at 37 °C (80 rpm) until an optical density (OD<sub>600 nm</sub>) of 0.5–0.8 was reached. The addition of isopropyl 1-thio-β-D-galactopyranoside (IPTG, 0.5 mM) induced protein expression. After 24 h post-induction, the cells were harvested by centrifugation (7,000 rpm, 30 min, 4 °C). For galectin purification, bacteria were suspended and sonicated on ice (two cycles, 30 s each, 52% amplitude). After removal of cell debris by centrifugation (15,000 rpm, 30 min, 4 °C), supernatant was filtered through 0.8 µm syringe filter. HisTrap™ HP 5 mL columns were used (GE Healthcare) according to manufacturer's instructions for galectin-3 purification. Eluted Gal-3 was dialyzed against phosphate buffered saline (PBS, 50 mM NaH<sub>2</sub>PO<sub>4</sub>, 150 mM NaCl, pH 7.5) supplemented with 2 mM ethylenediaminetetraacetic acid (EPBS) using SnakeSkin™ Dialysis Tubing (10 kDa MWCO, ThermoFisher Scientific).

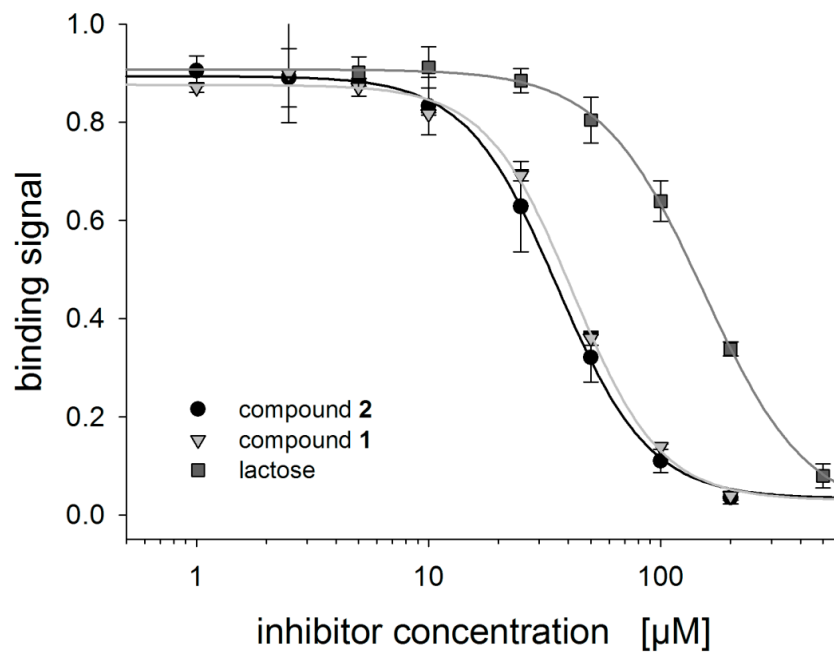


**Figure S5.** Competitive inhibition of Gal-3 binding to asialofetuin (ASF, coating amount: 5 pmol, 50 μL [0.1 μM] per well) using monovalent LacdiNAc (1), LacNAc (2) and lactose. Refer to Schemes S1 and S2 for compound composition. The respective IC<sub>50</sub> values are shown in Table 1.

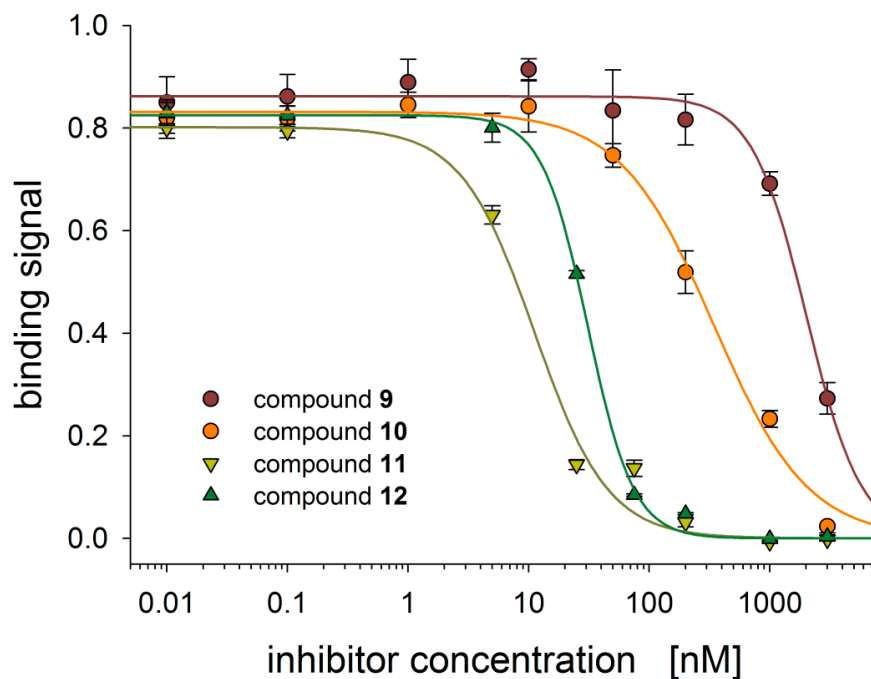


**Figure S6.** Inhibition of Gal-3 binding to immobilized ASF using BSA neo-glycoproteins 9-12 as inhibitors at indicated concentrations. Refer to Scheme S1 for compound composition. The respective IC<sub>50</sub> values are listed in Table 1 in the main text.

**Table S1.** Comparison of binding affinities of His<sub>6</sub>-tag Gal-3 and Gal-3-AVI in ELISA assays

Galectin-3 construct	$K_{d\text{ app}}$ [ $\mu\text{M}$ ], direct ELISA	$\text{IC}_{50}$ glycan [ $\mu\text{M}$ ], competitive ELISA	
	ASF	Lactose	LacdiNAc
His <sub>6</sub> -tag Gal-3	$5 \pm 1$	$137 \pm 27$	$42 \pm 2$
Gal-3-AVI	$4.8 \pm 0.2$	$110 \pm 4$	$43 \pm 4$

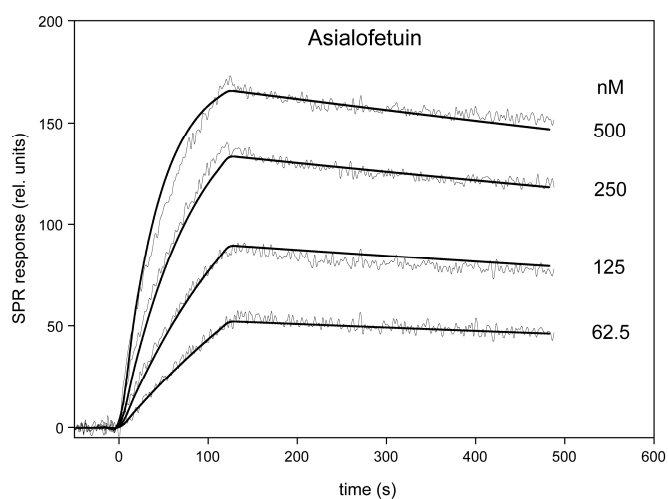


**Figure S7.** SPR kinetic binding analysis of the interactions between asialofetuin (ASF) and immobilized Gal-3-AVI. ASF was injected in parallel over the neutravidin-coated sensor chip coated with the biotinylated Gal-3-AVI at a flow rate of 30  $\mu\text{l}/\text{min}$ . The kinetic data were globally fitted by using a 1 : 1 Langmuir binding model. The fitted curves are superimposed as thin black line on top of the sensograms.

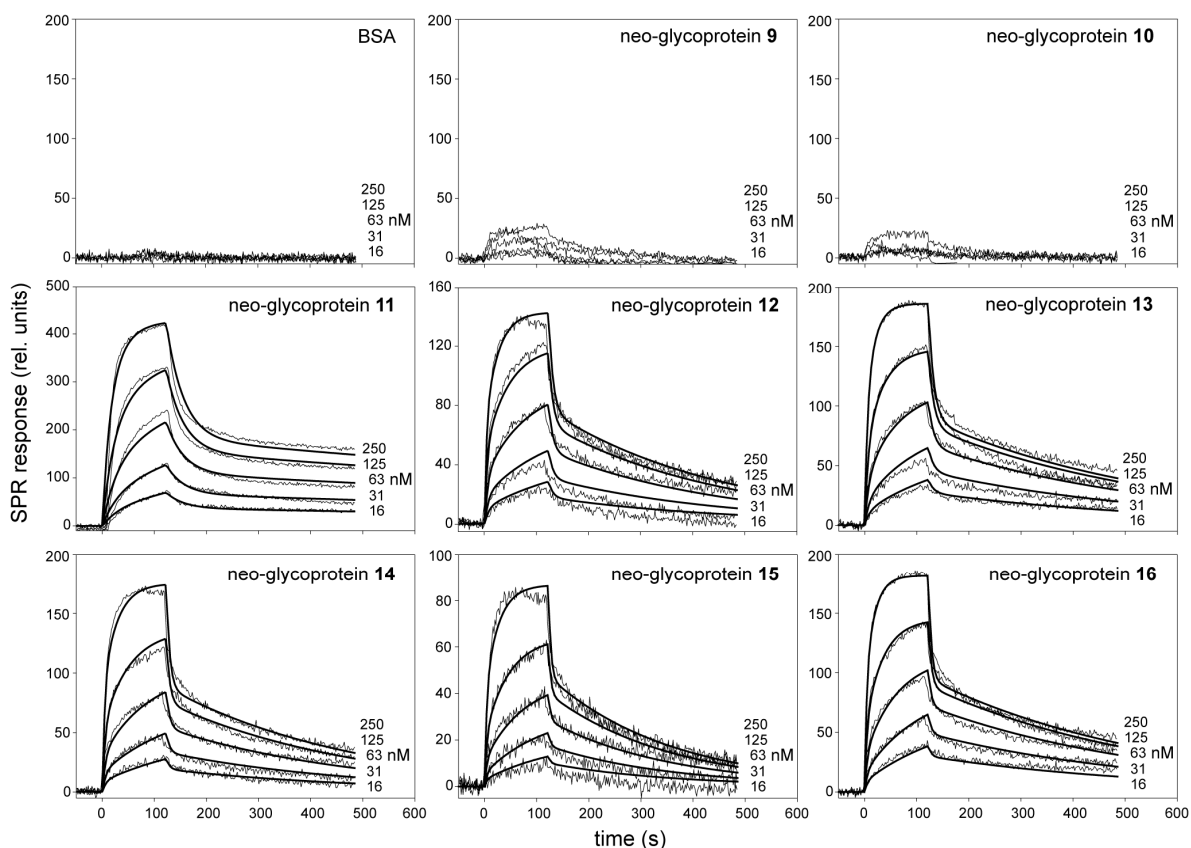


**Figure S8.** SPR kinetic binding analysis of the interactions between Gal-3 and immobilized neo-glycoproteins 9-16. The fitted curves (heterogenous ligand model) are superimposed on top of the sensograms.

**Table S2.** Kinetic and binding affinity constants for the interactions of Gal-3 with immobilized neo-glycoproteins 9-16.

Compound	$k_{a1}$ [ $M^{-1} s^{-1}$ ]	$k_{d1}$ [ $s^{-1}$ ]	$K_{D1}$ [M]	$k_{a2}$ [ $M^{-1} s^{-1}$ ]	$k_{d2}$ [ $s^{-1}$ ]	$K_{D2}$ [M]
<b>9</b>	N.D.	N.D.	N.D.	N.D.	N.D.	N.D.
<b>10</b>	N.D.	N.D.	N.D.	N.D.	N.D.	N.D.
<b>11</b>	$(1.2 \pm 0.8) \times 10^5$	$(4.5 \pm 2.1) \times 10^{-2}$	$(3.8 \pm 1.9) \times 10^{-7}$	$(1.0 \pm 1.1) \times 10^5$	$(9.4 \pm 3.8) \times 10^{-4}$	$(9.4 \pm 3.3) \times 10^{-9}$
<b>12</b>	$(9.3 \pm 4.3) \times 10^5$	$(1.3 \pm 1.1) \times 10^{-1}$	$(1.4 \pm 0.9) \times 10^{-7}$	$(1.5 \pm 1.2) \times 10^5$	$(2.9 \pm 1.2) \times 10^{-3}$	$(1.9 \pm 0.8) \times 10^{-8}$
<b>13</b>	$(4.1 \pm 2.5) \times 10^5$	$(2.1 \pm 1.1) \times 10^{-1}$	$(5.1 \pm 3.0) \times 10^{-7}$	$(1.8 \pm 1.2) \times 10^5$	$(2.1 \pm 1.3) \times 10^{-3}$	$(1.2 \pm 0.9) \times 10^{-8}$
<b>14</b>	$(3.3 \pm 1.7) \times 10^5$	$(1.6 \pm 1.2) \times 10^{-1}$	$(4.8 \pm 2.6) \times 10^{-7}$	$(1.5 \pm 1.0) \times 10^5$	$(2.7 \pm 1.2) \times 10^{-3}$	$(1.8 \pm 1.1) \times 10^{-8}$
<b>15</b>	$(3.9 \pm 2.1) \times 10^5$	$(2.4 \pm 1.3) \times 10^{-1}$	$(6.1 \pm 3.1) \times 10^{-7}$	$(1.9 \pm 1.5) \times 10^5$	$(4.1 \pm 1.9) \times 10^{-3}$	$(2.2 \pm 1.3) \times 10^{-8}$
<b>16</b>	$(3.5 \pm 1.9) \times 10^5$	$(1.8 \pm 1.4) \times 10^{-1}$	$(5.1 \pm 2.8) \times 10^{-7}$	$(2.1 \pm 1.4) \times 10^5$	$(2.3 \pm 1.1) \times 10^{-3}$	$(1.1 \pm 0.9) \times 10^{-8}$

## References

1. Blanchard, H.; Yu, X.; Collins, P.M.; Bum-Erdene, K. Galectin-3 inhibitors: a patent review (2008–present). *Expert Opin. Ther. Pat.* **2014**, *24*, 1053–1065, DOI:10.1517/13543776.2014.947961.
2. Collins, P.M.; Bum-Erdene, K.; Yu, X.; Blanchard, H. Galectin-3 interactions with glycosphingolipids. *J. Mol. Biol.* **2014**, *426*, 1439–1451, DOI:10.1016/j.jmb.2013.12.004.
3. Laaf, D.; Bojarová, P.; Pelantová, H.; Křen, V.; Elling, L. Tailored multivalent neo-glycoproteins: Synthesis, evaluation, and application of a library of galectin-3-binding glycan ligands. *Bioconjug. Chem.* **2017**, *28*, 2832–2840, DOI:10.1021/acs.bioconjchem.7b00520.
4. Böcker, S.; Laaf, D.; Elling, L. Galectin binding to neo-glycoproteins: LacDiNAc conjugated BSA as ligand for human galectin-3. *Biomolecules* **2015**, *5*, 1671–1696, DOI:10.3390/biom5031671.
5. Fischöder, T.; Laaf, D.; Dey, C.; Elling, L. Enzymatic synthesis of *N*-acetyllactosamine (LacNAc) type 1 oligomers and characterization as multivalent galectin ligands. *Molecules* **2017**, *22*, E1320, DOI:10.3390/molecules22081320.
6. Laaf, D.; Bojarová, P.; Mikulová, B.; Pelantová, H.; Křen, V.; Elling, L. Two-step enzymatic synthesis of  $\beta$ -D-*N*-acetylgalactosamine-(1→4)-D-*N*-acetylglucosamine (LacdiNAc) chitooligomers for deciphering galectin binding behavior. *Adv. Synth. Catal.* **2017**, *359*, 2101–2108, DOI:10.1002/adsc.201700331.
7. Kupper, C.E.; Rosencrantz, R.R.; Henssen, B.; Pelantová, H.; Thönes, S.; Drozdová, A.; Křen, V.; Elling, L. Chemo-enzymatic modification of *poly-N*-acetyllactosamine (LacNAc) oligomers and *N,N*-diacetyllactosamine (LacDINAac) based on galactose oxidase treatment. *Beilstein J. Org. Chem.* **2012**, *8*, 712–725, DOI:10.3762/bjoc.8.80.